Nav 1.7 and 1.8 Recordings on the IonFlux System

Introduction

The discovery that mutations in the SCN9A gene, which encodes the alpha subunit of NaV 1.7 Na^+ channels, are the almost certain cause of three different human genetic pain disorders has created a great deal of interest towards synthesizing subtype-specific novel analgesics (Drenth & Waxman, 2007; Momin & Wood, 2008). Clinical discoveries such as these, in rare inherited monogenic channelopathies, often point to general bio- molecular targets for therapeutic intervention in a broader spectrum of diseases. The pain disorders therefore highlight NaV 1.7, but also NaV 1.8 since this channel co- expresses with NaV 1.7 in dorsal root ganglia (DRG) and is the molecular effector of hyperexcitability, as drug targets of increased importance (Ogata & Ohishi 2002; Momin & Wood, 2008).

Until recently, screening of chemical entities targeting ion channels faced a bottle-neck caused by the relatively low throughput of patch-clamping. Patching requires specialized equipment and skilled practitioners, and is unwieldy for compound library-based screen- ing in the pharmaceutical industry. The advent of the automated patch clamp (APC) has nonetheless produced gains in ion channel screening throughput, although the available platforms still face difficulties presented by robotic scheduling leading to sub-optimal time resolution for compound applications and washout. In this application note we de- scribe the use of IonFlux, a novel microfluidics-based APC system, for recording Na+ current conducted by hNaV 1.7 and hNaV 1.8 channels expressed in HEK-293 cells, and block of I_{Na} by the local anesthetic lidocaine. The IonFlux system employs ensemble recording arrays consisting of twenty or thirty cells voltage clamped in parallel at 16 or 64 recording sites, each exposed to as many as eight different compounds or concentrations in a 96-well or 384-well format. The IonFlux instrument incorporates no internal robotics and offers rapid, microfluidic compound applications. It has a compact “plate reader” footprint suitable for bench-top operation.

Figure 1: The IonFlux system utilizes a “plate reader” format to simplify workflow and increase throughput. Systems are available with 16 and 64 amplifiers. Throughput of 10,000 data points per day can be achieved.

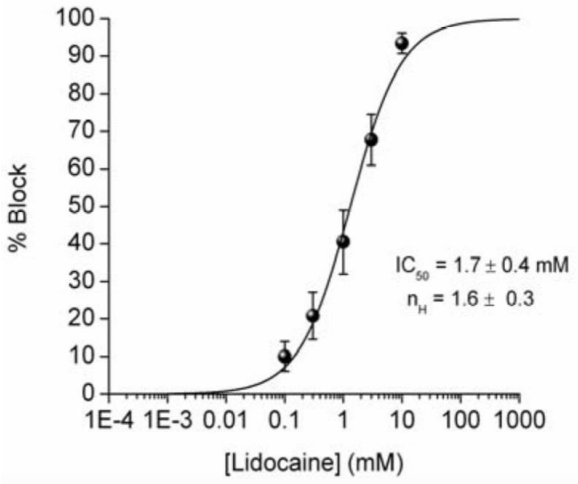

Figure 2: Superimposed current-versus-time plots during cumulative lidocaine applications at concentrations ranging between 0.1 and 10 mM (top, screen capture). The dose-response relationship is shown below, with mean Hill fit parameters obtained from the ensemble recordings on a single IonFlux plate (N = 11 ensembles)

Methods

Preparation of cells

HEK-293 cells expressing the channels of interest were utilized (Millipore PrecisION™ Recombinant Cell Lines, hNav1.7-HEK (Cat No. CYL3011) and hNav1.8/β_1-HEK (Cat No. CYL3025)). The cells were cultured according to standard operating protocols provided. Briefly, maintenance was in Glutamax DMEM/F12 medium with 10% FBS plus selection / expression enhancement agents at 37ºC, in a humidified, 5% CO2 atmosphere. The cultures never exceeded 80% confluence. Cells were released from culture flasks using Detachin (Genlantis, San Diego, CA, Cat# T100100) and after washing and gentle trituration, a suspension was produced in extracellular solution (ECS) containing 5 million cells per ml. Aliquots of cell suspension were loaded into wells on the IonFlux plate.

Experimental Procedures

The IonFlux plate layout consists of units of twelve wells; two wells contain intracellular solution (cytosolic compartment), one contains ECS plus cells, eight contain ECS plus compounds of interest, and one well is for waste collection (for further information see www.fluxionbio.com). Cells are captured from suspension by applying suction to microscopic channels in ensemble recording arrays. Cell capture is monitored by means of the electrical resistance across the recording array. Once the array is fully occupied, the applied suction breaks the cell membranes of captured cells, establishing whole cell voltage clamp. For compound applications, pressure is applied to the appropriate compound well, introducing the compound into the extracellular solution rapidly flowing over the cells.

For recording Na^+ currents, cell arrays were voltage clamped at a holding potential of -80 mV, stepped to -120 mV for 50 ms to maximize channel availability, and then to -10 mV to open the Na+ channels (50 ms). In some experiments the final step was to -50 mV (or -70 mV), followed by ten to twelve 10 mV increments. All voltage protocols were applied at 1 Hz. Leak current was compensated online using pairs of small depolarizations (-20 mV at 20 Hz) and the series resistance attributable to the ensemble recording array (approximately 0.8 MW) was compensated electronically, as was stray capacitance. Ionic currents were sampled at 10 kHz.

Solutions

Extracellular solution (ECS) contained (mM): NaCl 137, KCl 4, MgCl2 1, CaCl2 1.8, HEPES 20, dextrose 10 brought to pH 7.4 using NaOH. The intracellular solution contained (mM): CsF 100, CsCl 45, HEPES 10, NaCl 5, EGTA 5 brought to pH 7.2 using CsOH.

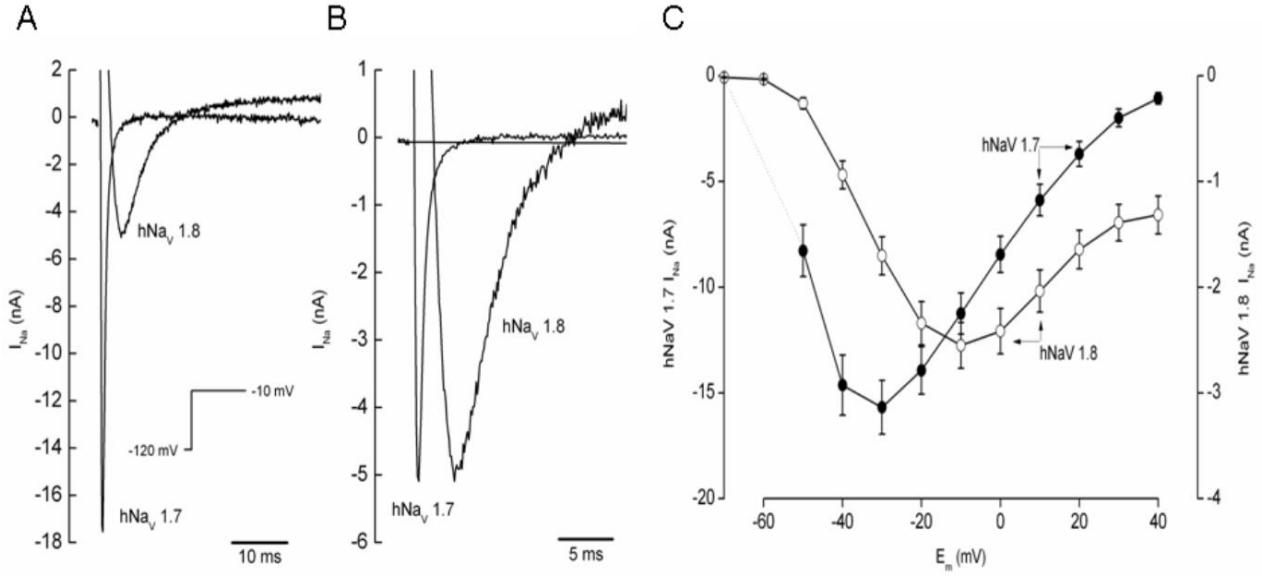

Figure 3: A: Superimposed individual ensemble Na+ currents from cells expressing hNaV 1.7 and hNaV 1.8 channels (inset shows voltage protocol). **B:** Currents of panel A scaled to match peak INa to emphasise the kinetic differences. **C:** Mean current-versus- voltage plots of INa for the two hNaV channels. Peak INa for hNaV 1.7 (N = 31 ensembles) lies at a more hyperpolarized membrane potential than for hNaV 1.8 (N= 31). Note also the more sensitive ordinate scale for hNaV 1.8 (right axis).

A stock solution containing 10 mM lidocaine in ECS was diluted in a three-fold dilution series for dose-response experiments.

Results

Voltage dependent properties of hNaV currents

To determine the current-vs-voltage relationships for hNaV 1.7 and 1.8, square voltage pulses were applied to cell ensembles. Figure 3A shows superimposed IonFlux recordings of two individual ensemble currents indicating the large differences in I_{Na} amplitude and kinetics for the two channels. After scaling to match peak I_{Na} (Figure 3B), the characteristic kinetics of the two currents are clear, with hNaV 1.7 current activating and inactivating very rapidly compared to hNaV 1.8 current. The mean amplitude of hNaV 1.7 ensemble currents was - 12.3 ± 1.0 nA (N= 53 ensembles), while that of hNaV 1.8 was -2.9 ± 0.3 nA (N= 32). This large discrepancy most likely reflects the diffi- culty of producing high expression levels of hNaV 1.8 in mammalian heterologous systems (Zhao et al., 2007).

Comparative pharmacology of hNav currents

Since our primary objective in developing IonFlux has been to provide a high throughput screening tool for use in ion channel drug development, we further

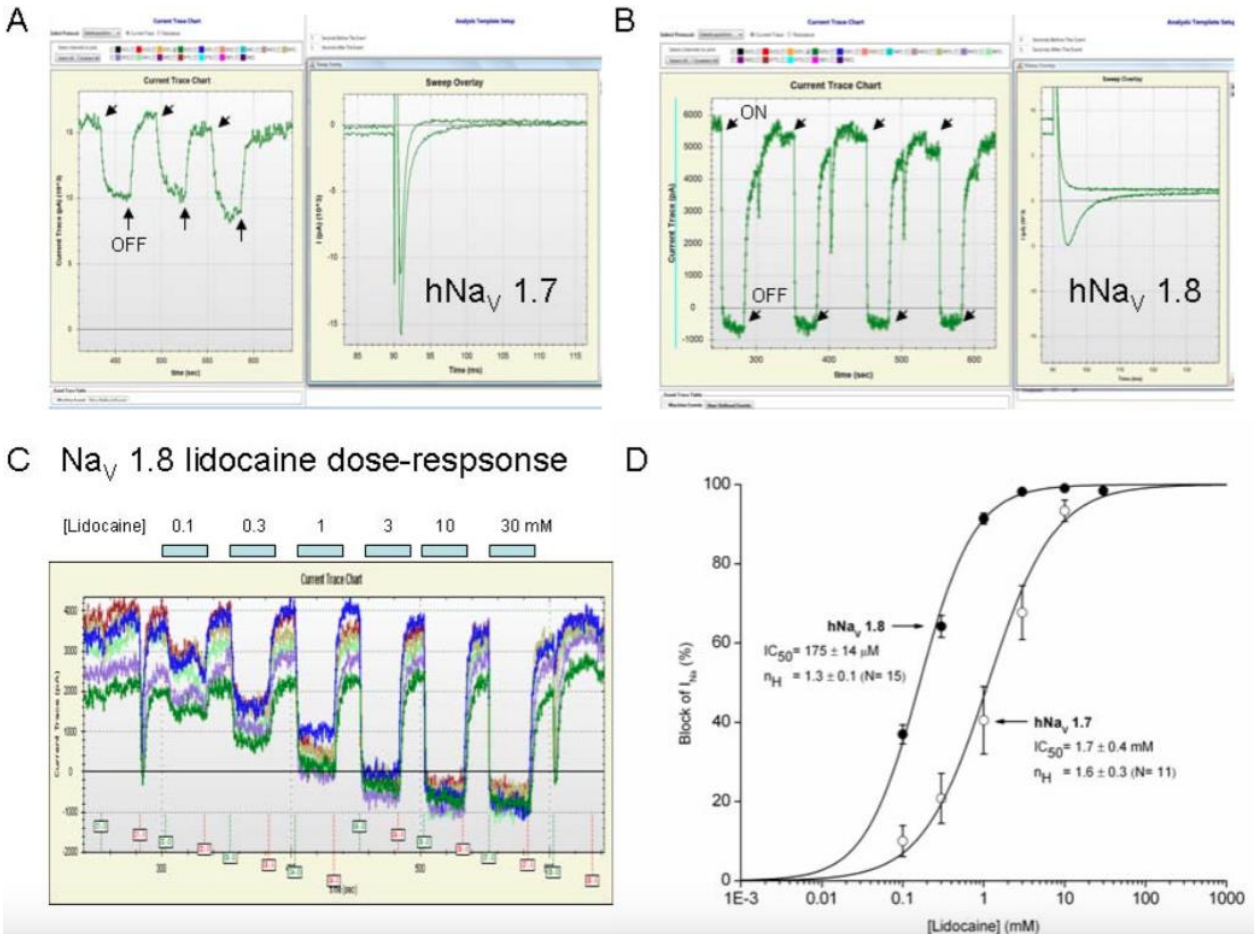

Figure 4: A: Representative screen-shot image of hNaV 1.7 ensemble Na+ currents (right display box) in the presence and absence of 3 mM lidocaine, together with current-versus-time plots (left display box) obtained by cursor measurements during three successive 3 mM lidocaine applications separated by washouts, indicated by arrows. **B:** Equivalent results to panel A from cells expressing NaV 1.8 channels, with ensembles given four successive applications of 3 mM lidocaine (arrows) with washouts in-between. The individual NaV 1.8 currents (right display box) show that lidocaine block was considerably greater for this channel than for NaV 1.7. **C:** Screen-shot of the current vs time screen in a lidocaine dose-response experiment for hNaV 1.8, with the lidocaine applications shown as colored bars at the top. **D:** Lidocaine mean dose-response relationships for hNaV 1.8 (curve to left) and hNaV 1.7 (curve to right), with mean Hill fit parameters for both NaV channels.

investigated the comparative pharmacology of hNaV 1.7 and 1.8 channels. Figures 4A and 4B show screen capture images from the IonFlux data monitor depicting representative experiments to block ensemble hNaV currents using rapid applications of 3 mM lidocaine in ECS. From the current versus time plots (left side of each panel), it can be easily appreciated that the onset of lidocaine block was rapid for both channels, as was the recovery of I_{Na} during washout of the local anesthetic. Lidocaine blockade was also completely reversible and this was highly repeatable for both of the hNaV subtypes. Moreover, the extent of lidocaine block can be seen to be sub-type specific, since 3 mM lidocaine blocked a fraction of I_{Na} in cells expressing the hNaV 1.7 channels (Figure 4A), while hNaV 1.8 current was almost completely suppressed (Figure 4B). An example of a lidocaine dose-response experiment for this channel is shown as a screen-shot from IonFlux software in Figure 4C, where increasing concentrations were applied to a set of cell ensembles with washout between each application. Lidocaine hNaV sub-type selectivity is strongly reflected in the lidocaine dose-response curves shown in Figure 4D. Based on the ensemble current measurements, hNaV 1.8 channels were found to be an order or magnitude more sensitive to lidocaine (IC50 = 175 ± 14 @M, nH = 1.3 ± 0.1, N = 15 ensembles) than are hNaV 1.7 channels (IC50 = 1.7 ± 0.4 mM, nH = 1.6 ± 0.3, N = 11 ensembles). In a previous comparative study, the relative sensitivities to this local anesthetic were found to differ by at least a factor of five, with NaV 1.8 channels being more sensitive (Chevrier, Vijayaragavan & Chahine, 2004). The smaller sensitivity differential observed in that study may relate to the expression of the channels of interest in Xenopus oocytes instead of mammalian cells, and also since the Hill fit for the NaV 1.8 results seems to be somewhat less well-defined than ours.

Discussion

These results validate IonFlux recordings of hNaV 1.7 and 1.8 currents and block by lidocaine. The IonFlux instrument applies an averaged voltage correction for series resistance that will not exactly compensate series resistance in each individual voltage-clamped cell; nonetheless, the observed lack of excessive steepness in the negative IV slopes (Figure 3B) suggests that voltage control was adequately maintained during these experiments. Such findings are highly comparable to population-based NaV recordings made on other platforms (Finkel et al., 2006), supporting the use of IonFlux in the drug screening arena.

The usefulness of IonFlux as a screening and drug-development tool is considerably reinforced by the lidocaine blockade results shown in Figure 4. In Figure 4D, lidocaine dose-response curves rapidly recorded in parallel at multiple recording zones across one IonFlux consumable plate are compared. The lidocaine IC50 values were internally consistent and comparable to published findings for each of the NaV channels, and sub-type selectivity was clearly demonstrated. Such performance emphasizes the gains in throughput and simplicity provided by the IonFlux instrument.

There is a continuing need for enhanced high throughput screening against targets like hNaV 1.7 and 1.8. It appears that pain disorders attributable to missense mutations causing gains in NaV function (PE and PEPD) can be reduced by selectively blocking NaV 1.7 or 1.8 channels. By avoiding the side effects of conventional Na+ channel blockers, novel selective agents can potentially find multiple uses in pain management. This application note provides results supporting an important role for IonFlux in future drug discovery campaigns aimed at these and other diverse drug targets.

References

- Chevrier P, Vijayaragavan K & Chahine (2004). *Brit. J. Pharmacol*. 142, 576-84
- Drenth JPH & Waxman SG (2007). *J. Clin. Investigation* 117, 3603-9.
- Finkel A, Wittel A, Yang N, Handran S, Hughes J & Constantin J (2006). *J. Biomolec. Screening* 11, 488-96.
- Momin A & Wood JN (2008). *Curr. Opin. Neurobiol*. 18, 383-8.
- Ogata N & Ohishi Y (2002). *Jpn J. Pharmacol*. 88, 365-377.
- Sheets PL, Jackson JO, Waxman SG, Dib-Hajj S & Cummins TR (2007). *J. Physiol.* 581, 1019-31
- Sheets PL, Heers C, Stoehr T & Cummins TL (2008). *J. Pharmacol. Exp. Ther.* 326, 89-99